Journal of Integer Sequences, Vol. 28 (2025),
Article 25.7.3

Enumeration of Coronas for Lozenge Tilings

Craig Knecht
Harris Lane
Gallatin, TN 37066
USA
craigknecht03@gmail.com

Feihu Liu[1] and Guoce Xin
School of Mathematical Sciences
Capital Normal University
Beijing, 100048
China
feihu.liu@cnu.edu.cn
guoce_xin@163.com

Abstract

We study the enumeration of coronas. This counting problem concerns two specific types of lozenge tilings. Exact closed-form formulas for these were conjectured in sequences A380346 and A380416 of the OEIS. We prove these conjectures by employing the weighted adjacency matrix. Furthermore, we extend these results to a general setting.

1 Introduction

We begin by introducing basic definitions [4]. The *triangular lattice* is a tiling of the Euclidean plane $\mathbb{R}^2$ by unit equilateral triangles. A *lozenge* (or *diamond*) consists of two adjacent unit triangles sharing an edge. A *region* in this lattice is a finite set of unit triangles.

[1]Corresponding author.

A *lozenge tiling* of a region R is a partition of R into lozenges; that is, a covering with no gaps or overlaps.

Unit equilateral triangles have two possible orientations: upwards-pointing and downwards-pointing. Consequently, lozenges admit three orientations: left-tilted, right-tilted, and vertical (Figure 1).

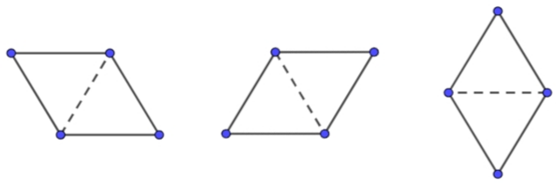

Figure 1: Orientations of lozenges: left-tilted, right-tilted, and vertical.

The central problem is enumerating lozenge tilings of a given region R. This is a well-studied topic in combinatorics, known for elegant formulas and ingenious arguments [2, 4, 8, 12]. Various enumeration methods exist, such as Kuo's graphical condensation [5], and determinant-based approaches via nonintersecting lattice paths [1]. Lai and collaborators have made significant contributions through a series of works [6, 7, 10, 9, 11, 3].

This work is motivated by recent studies on corona enumerations [13, A380346,A380416]. The term "corona" originates from Knecht. For a regular hexagon H, a *corona of* H is a lozenge tiling strictly along its boundary without extraneous tiles. Figures 2(a–b) illustrate coronas of side lengths 1 and 2, while Figures 2(c–d) fail to be coronas. Figure2(c) contains a redundant lozenge e. Figure2(d) has a gap at the bottom-left corner. Let $H(n)$ denote the number of coronas for a regular hexagon of side length n.

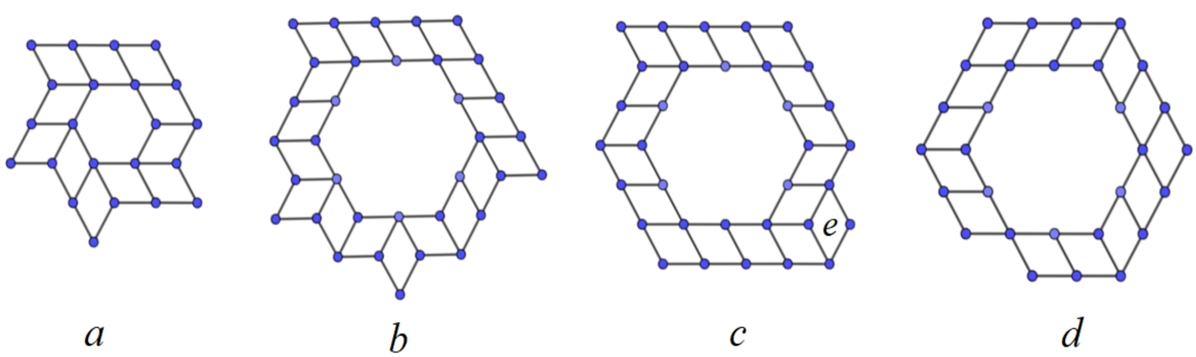

Figure 2: Coronas and non-coronas of a regular hexagon H.

Our first result establishes an exact formula for $H(n)$, confirming the following conjecture.

Theorem 1. (Conjectured in [13, A380346]) *Let $n \in \mathbb{N}$ and $H(n)$ be the number of coronas of a regular hexagon of side length n. Coronas utilize exactly one of four possible lozenge* *counts:* $6n+3$, $6n+4$, $6n+5$, *or* $6n+6$. *Define* $h_i(n)$ *as the number of corona tilings with* $6n+2+i$ *lozenges for* $1 \le i \le 4$. *Then we have*

$$h_1(n) = 2, \quad h_2(n) = 9(n+1)^2, \quad h_3(n) = 6(n+1)^4, \quad h_4(n) = (n+1)^6,$$

and

$$H(n) = \sum_{i=1}^{4} h_i(n) = n^6 + 6n^5 + 21n^4 + 44n^3 + 60n^2 + 48n + 18.$$

Similarly, given a diamond D with 60° and 120° angles, a *corona of* D is a lozenge tiling along the boundary of D that uses no additional lozenges. For example, Figure3(p) shows a corona of a diamond D of side length 1; Figure3(q) shows a corona of a diamond D of side length 2. However, Figure3(u) is not a corona due to the redundant lozenge w; and Figure3(v) is also not a corona because a lozenge is missing in the bottom right corner. We denote by $D(n)$ the number of coronas of a diamond of side length n.

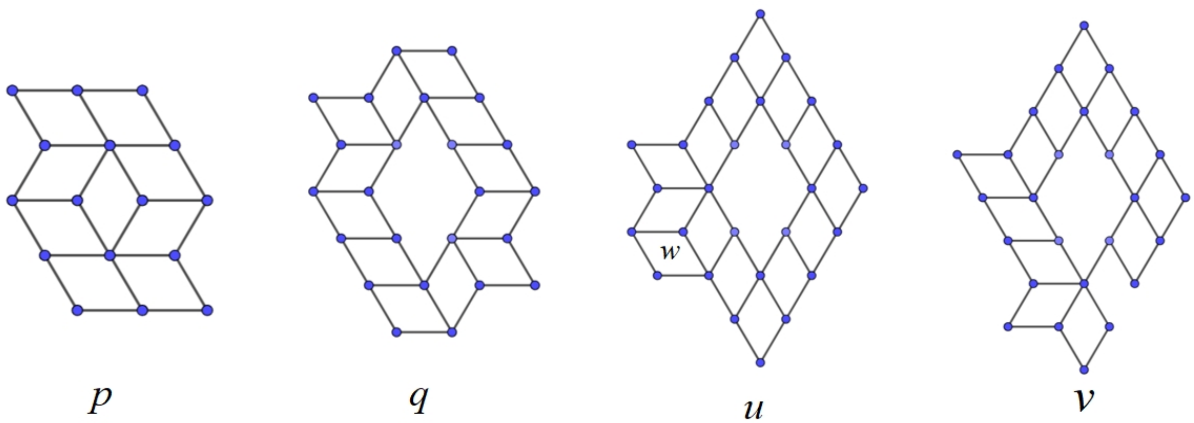

Figure 3: Coronas and non-coronas of a diamond D.

Our second result provides an exact closed formula for $D(n)$.

Theorem 2. (Conjectured in [13, A380416]) *Let* $n \in \mathbb{N}$ *and* $D(n)$ *denote the number of coronas of a diamond of side length* n. *Then the number of lozenges in any corona for a diamond of side length* n *is one of four values:* $4n+3$, $4n+4$, $4n+5$, *or* $4n+6$. *Let* $d_i(n)$ *be the number of corona tilings using* $4n+2+i$ *lozenges for* $1 \le i \le 4$. *Then*

$$d_1(n) = 2, \quad d_2(n) = (2n+3)^2, \quad d_3(n) = 2(n+1)^2(2n+3), \quad d_4(n) = (n+1)^4,$$

and consequently,

$$D(n) = \sum_{i=1}^{4} d_i(n) = n^4 + 8n^3 + 24n^2 + 32n + 18.$$

Inspired by Knecht's work, we extend the study of coronas to shapes with modified side lengths. We relax the requirement that all sides of the regular hexagon H and diamond D are equal, requiring only that opposite sides have equal length. This preserves their interior angles. The resulting shapes are called a *centrally symmetric hexagon* and a *parallelogram*, denoted by $\overline{H}$ and $\overline{D}$, respectively; see Figure 13. Our third result establishes exact closed formulas for the number of coronas of $\overline{H}$ and $\overline{D}$ in Theorems 7 and 8, respectively. These generalize Theorems 1 and 2.

The paper is organized as follows. Section 2 presents preliminary results on the enumeration of walks in graphs. We prove the main theorems in Section 3. Finally, Section 4 contains the extensions of Theorems 1 and 2.

2 Preliminary: walks in graphs

This section introduces fundamental concepts regarding walks in graphs [14, Chapter 1], establishing results essential for proving our main theorems.

A *graph* $G = (V, E)$ consists of a *vertex set* $V = \{v_1, v_2, \ldots, v_m\}$ and an *edge set* E, where each edge is an unordered pair of distinct vertices. We follow the notation of [14, Chapter 1]. The *adjacency matrix* of G is the $m \times m$ symmetric matrix $A(G)$ whose (i, j)-entry a_{ij} equals the number of edges between vertices v_i and v_j.

A *walk* in G of *length* ℓ from vertex u to v is a sequence $v_1, e_1, v_2, e_2, \ldots, v_\ell, e_\ell, v_{\ell+1}$ such that $v_i \in V$, $e_j \in E$, the vertices of e_i are v_i and v_{i+1}, for $1 \leq i \leq \ell$, and $v_1 = u$, $v_{\ell+1} = v$.

Lemma 3. [14, Theorem 1.1] *For any positive integer ℓ, the (i, j)-entry of $A(G)^\ell$ equals the number of walks of length ℓ from v_i to v_j in G.*

A *closed walk* is a walk that starts and ends at the same vertex. The number of closed walks of length ℓ starting at v_i is therefore $(A(G)^\ell)_{ii}$.

Corollary 4. [14, Chapter 1] *The total number $f_G(\ell)$ of closed walks of length ℓ is given by*

$$f_G(\ell) = \sum_{i=1}^{m} (A(G)^\ell)_{ii} = \operatorname{tr}(A(G)^\ell),$$

where tr *denotes the matrix trace (that is, the sum of main diagonal entries).*

3 Proofs of the main theorems

Consider a regular hexagon H with side length n, whose six corners are labeled $1, 2, 3, 4, 5, 6$ as shown in Figure 4. Examination of the coronas reveals five possible lozenge configurations at each corner of H. The five states at corner 1 are displayed in Figure 5, containing 3, 3, 4, 2, and 3 lozenges respectively. By rotational symmetry, the states at the remaining corners

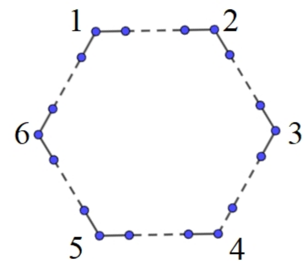

Figure 4: A regular hexagon H.

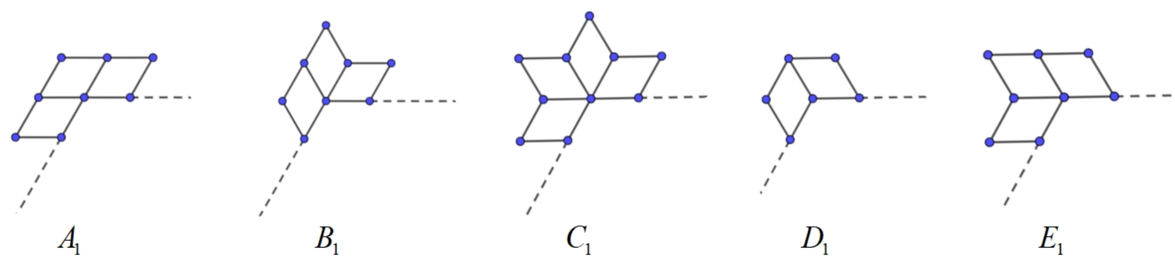

Figure 5: The five states at corner 1.

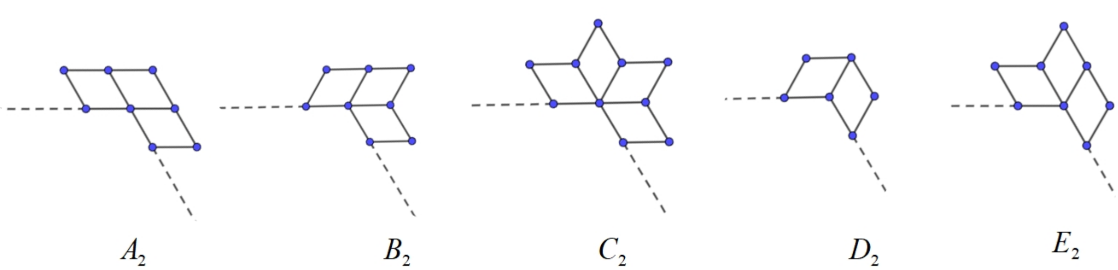

Figure 6: The five states at corner 2.

are rotations of those at corner 1. For example, Figure 6 illustrates the corresponding states at corner 2.

For the corona of H, there are $n+1$ possible lozenge states along the edge between corners 1 and 2, as depicted in Figure 7. The states along the other edges are obtained by rotation of these $n+1$ configurations. In Figure 7, states Q and K each contain $n-2$ lozenges, while states L_i $(1 \leq i \leq n-1)$ each contain $n-1$ lozenges.

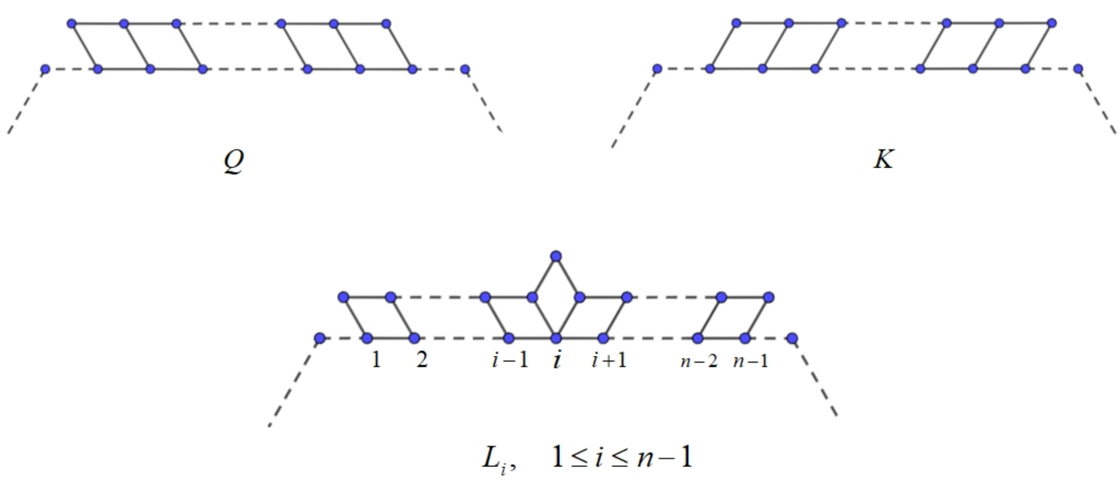

Figure 7: The $n+1$ states on the side.

We now prove Theorem 1.

Proof of Theorem 1. By the preceding discussion, corners 1 and 2 are connected via the $n+1$ states in Figure 7. We thus construct the bipartite graph shown in Figure 8, where an edge between two vertices indicates that the corresponding corners can be concatenated through these states. For example, state D_1 connects to A_2, C_2, and E_2 via state Q, and to B_2 and D_2 via states L_i $(1 \leq i \leq n-1)$. Specifically, there are $n-1$ multi-edges between D_1 and B_2, and similarly between D_1 and D_2.

The weighted adjacency matrix M of the graph in Figure 8 is given by:

$$M = \begin{array}{c} \\ A_1 \\ B_1 \\ C_1 \\ D_1 \\ E_1 \end{array} \begin{array}{c} \begin{array}{ccccc} A_2 & B_2 & C_2 & D_2 & E_2 \end{array} \\ \begin{pmatrix} 0 & x^{3+n-2} & 0 & x^{2+n-2} & 0 \\ 0 & x^{3+n-2} & 0 & x^{2+n-2} & 0 \\ 0 & x^{3+n-2} & 0 & x^{2+n-2} & 0 \\ x^{3+n-2} & (n-1)x^{3+n-1} & x^{4+n-2} & (n-1)x^{2+n-1} & x^{3+n-2} \\ x^{3+n-2} & (n-1)x^{3+n-1} & x^{4+n-2} & (n-1)x^{2+n-1} & x^{3+n-2} \end{pmatrix} \end{array}. \quad ,$$

where the exponent r in the weight x^r denotes the total number of lozenges in corner 2 and the connecting edge from Figure 7. By Corollary 4, it suffices to compute the trace of M^6.

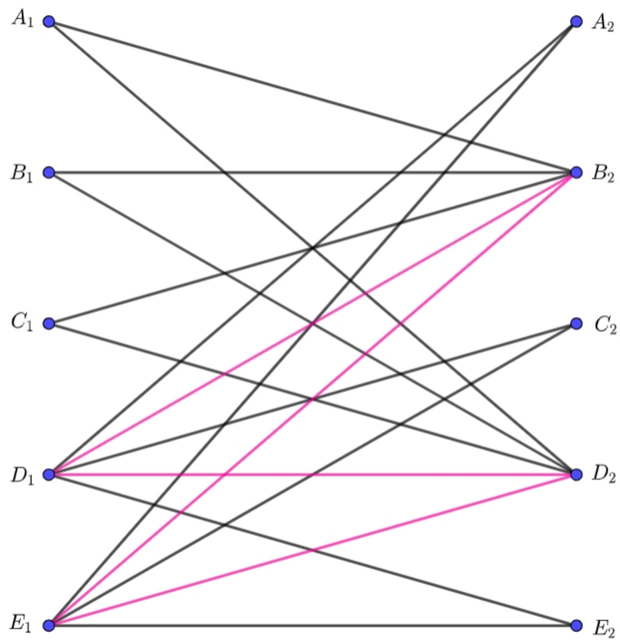

Figure 8: The bipartite graph in the proof of Theorem 1.

Direct matrix multiplication yields

$$\sum_{i=1}^{5}(M^6)_{ii} = \mathrm{tr}(M^6) = 2x^{6n+3} + 9(n+1)^2x^{6n+4} + 6(n+1)^4x^{6n+5} + (n+1)^6x^{6n+6}.$$

This completes the proof. □

We assume familiarity with generating functions (see [15, Chapter 1]).

Corollary 5. *Let n be a nonnegative integer, and let $H(n)$ denote the number of coronas of a regular hexagon of side length n. The generating function for $H(n)$ is*

$$\sum_{n=0}^{\infty} H(n)x^n = \frac{2x^6 + 4x^5 + 114x^4 + 220x^3 + 290x^2 + 72x + 18}{(1-x)^7}.$$

Now we consider the coronas of a diamond D. Given a diamond D of side length n, denote its four corners by 1, 2, 3, and 4 (see Figure 9). Examination of these coronas reveals that there exist 8 possible states for lozenges at corner 1, as illustrated in Figure 10, and 5 states at corner 2, shown in Figure 11. The states at corners 3 and 4 are obtained by rotating those at corners 1 and 2 by 180°, respectively. Analogous to corner 1 (Figure 10), the states for lozenges at corner 3 are denoted A_3, B_3, C_3, D_3, E_3, F_3, I_3, J_3. For a corona of diamond D with side length n (identical to Figure 7), there are $n+1$ possible states for the lozenges between corner 1 and corner 2.

We now prove Theorem 2.

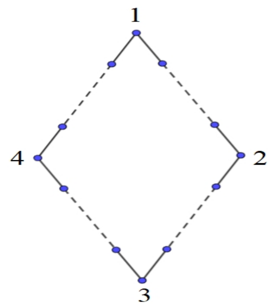

Figure 9: A diamond D.

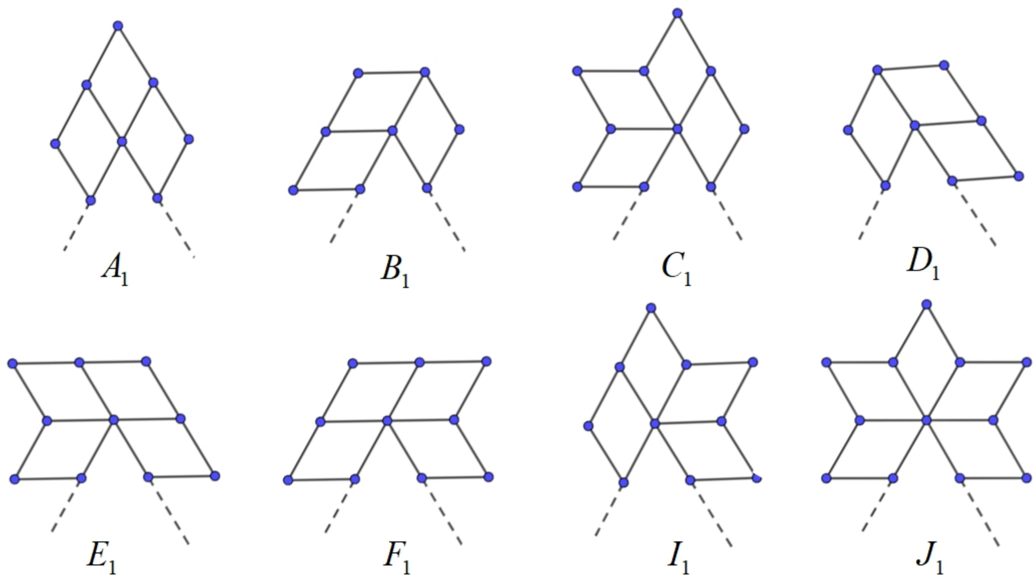

Figure 10: The eight states at corner 1.

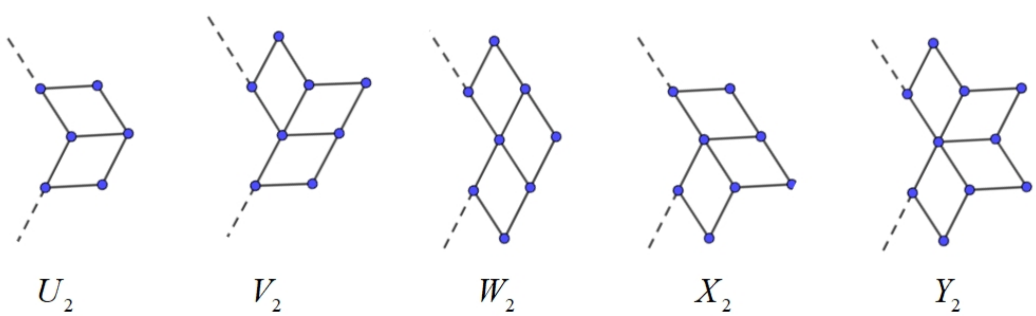

Figure 11: The five states at corner 2.

Proof of Theorem 2. Similar to the proof of Theorem 1, we construct the graph depicted in Figure 12. An edge between two vertices in this graph signifies that the corresponding states at corner 1 and corner 2 (or corner 2 and corner 3) can be concatenated via the configurations shown in Figure 7. For instance, state A_1 connects to states V_2, W_2, and Y_2 through state Q, and to states U_2 and X_2 through the states L_i $(1 \le i \le n-1)$. More precisely, there are $n-1$ multi-edges between A_1 and U_2, and similarly between A_1 and X_2.

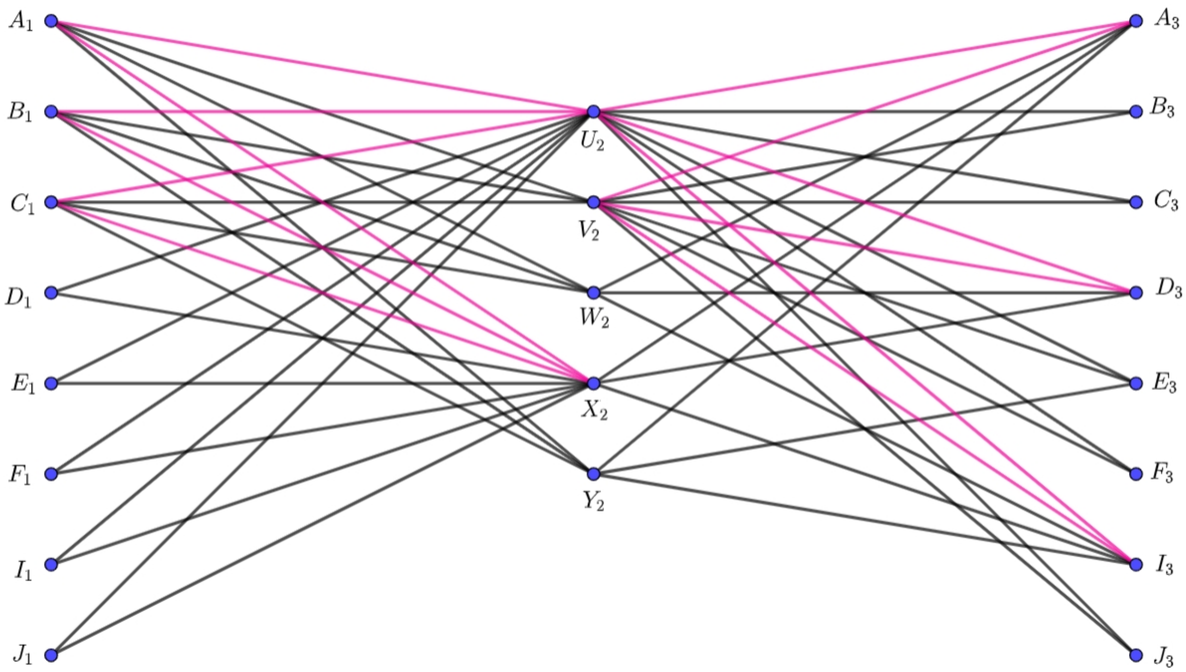

Figure 12: The graph in the proof of Theorem 2.

We construct the following two weighted adjacency matrices R and T:

$$R = \begin{array}{c} \\ A_1 \\ B_1 \\ C_1 \\ D_1 \\ E_1 \\ F_1 \\ I_1 \\ J_1 \end{array} \begin{array}{c} \begin{array}{ccccc} U_2 & V_2 & W_2 & X_2 & Y_2 \end{array} \\ \left(\begin{array}{ccccc} (n-1)x^{2+n-1} & x^{3+n-2} & x^{3+n-2} & (n-1)x^{3+n-1} & x^{4+n-2} \\ (n-1)x^{2+n-1} & x^{3+n-2} & x^{3+n-2} & (n-1)x^{3+n-1} & x^{4+n-2} \\ (n-1)x^{2+n-1} & x^{3+n-2} & x^{3+n-2} & (n-1)x^{3+n-1} & x^{4+n-2} \\ x^{2+n-2} & 0 & 0 & x^{3+n-2} & 0 \\ x^{2+n-2} & 0 & 0 & x^{3+n-2} & 0 \\ x^{2+n-2} & 0 & 0 & x^{3+n-2} & 0 \\ x^{2+n-2} & 0 & 0 & x^{3+n-2} & 0 \\ x^{2+n-2} & 0 & 0 & x^{3+n-2} & 0 \end{array} \right) \end{array} . \quad ,$$

and

$$T = \begin{array}{c} \\ U_2 \\ V_2 \\ W_2 \\ X_2 \\ Y_2 \end{array} \begin{array}{c} \begin{array}{cccccccc} A_3 & B_3 & C_3 & D_3 & E_3 & F_3 & I_3 & J_3 \end{array} \\ \begin{pmatrix} (n-1)x^{n+2} & x^{n+1} & x^{n+2} & (n-1)x^{n+2} & x^{n+2} & x^{n+2} & (n-1)x^{n+3} & x^{n+3} \\ (n-1)x^{n+2} & x^{n+1} & x^{n+2} & (n-1)x^{n+2} & x^{n+2} & x^{n+2} & (n-1)x^{n+3} & x^{n+3} \\ x^{n+1} & 0 & 0 & x^{n+1} & 0 & 0 & x^{n+2} & 0 \\ x^{n+1} & 0 & 0 & x^{n+1} & 0 & 0 & x^{n+2} & 0 \\ x^{n+1} & 0 & 0 & x^{n+1} & 0 & 0 & x^{n+2} & 0 \end{pmatrix} \end{array}.$$

By Corollary 4, we need only compute the trace of $(R \cdot T)^2$. After detailed matrix multiplication, we obtain

$$\begin{aligned} \sum_{i=1}^{8}((R\cdot T)^2)_{ii} &= \operatorname{tr}((R\cdot T)^2) \\ &= 2x^{4n+3} + (2n+3)^2x^{4n+4} + 2(n+1)^2(2n+3)x^{4n+5} + (n+1)^4x^{4n+6}. \end{aligned}$$

This completes the proof. □

Corollary 6. *For $n \in \mathbb{N}$, let $D(n)$ denote the number of coronas of a diamond D with side length n. The generating function for $D(n)$ is given by*

$$\sum_{n\geq 0} D(n)x^n = \frac{3x^4 - 13x^3 + 23x^2 - 7x + 18}{(1-x)^5}.$$

4 An extension for the coronas

We now consider an extension pertaining to the coronas. Specifically, we modify the side lengths of a regular hexagon H or a diamond D while preserving their interior angles. More precisely, the *centrally symmetric hexagon* $\overline{H}$ is defined as shown on the left of Figure 13. It has three pairs of opposite sides with lengths $n_1, n_2, n_3 \in \mathbb{N}$ and all interior angles equal to 120°. The *parallelogram* $\overline{D}$ is defined by the right of Figure 13. It has two pairs of opposite sides with lengths $n_1, n_2 \in \mathbb{N}$ and interior angles of 60°, 120°, 60°, and 120° (in cyclic order).

Note that when $n_3 = 0$, the centrally symmetric hexagon $\overline{H}$ reduces to the parallelogram $\overline{D}$.

Given a centrally symmetric hexagon $\overline{H}$, a *corona of* $\overline{H}$ is a lozenge tiling along the edges of $\overline{H}$ without utilizing any additional lozenges. The number of distinct coronas of $\overline{H}$ is denoted by $\overline{H}(n_1, n_2, n_3)$.

Theorem 7. *Let $n_1, n_2, n_3 \in \mathbb{N}$. Let $\overline{H}(n_1, n_2, n_3)$ denote the number of coronas of a centrally symmetric hexagon $\overline{H}$. There are exactly four cases corresponding to the number of lozenges in a corona of $\overline{H}$, namely $2(n_1+n_2+n_3)+3$, $2(n_1+n_2+n_3)+4$, $2(n_1+n_2+n_3)+5$, and*

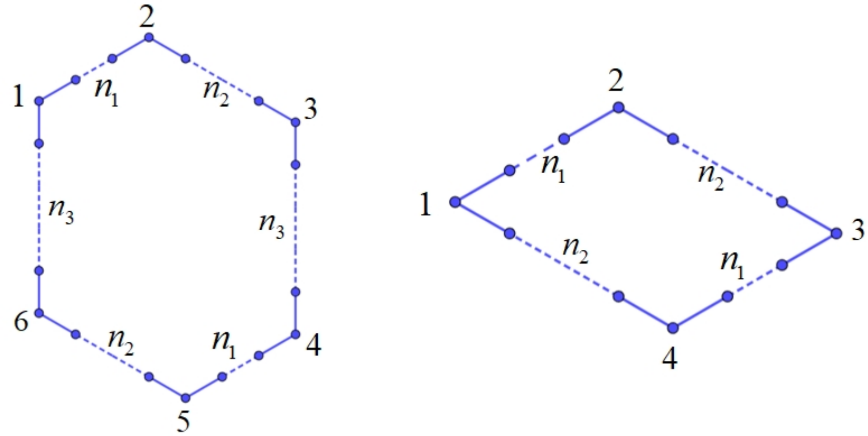

Figure 13: A centrally symmetric hexagon $\overline{H}$ and a parallelogram $\overline{D}$.

$2(n_1+n_2+n_3)+6$. *For* $1 \le i \le 4$, *let* $\overline{h}_i(n)$ *be the number of corona tilings corresponding to the number of lozenges* $2(n_1+n_2+n_3)+2+i$. *Then we have*

$$\overline{h}_1(n) = 2, \qquad \overline{h}_3(n) = 2(n_1+1)(n_2+1)(n_3+1)(n_1+n_2+n_3+3),$$
$$\overline{h}_2(n) = (n_1+n_2+n_3+3)^2, \qquad \overline{h}_4(n) = (n_1+1)^2(n_2+1)^2(n_3+1)^2.$$

Moreover, we have

$$\overline{H}(n_1,n_2,n_3) = \sum_{i=1}^{4} \overline{h}_i(n) = \big((n_1+1)(n_2+1)(n_3+1) + (n_1+n_2+n_3+3)\big)^2 + 2.$$

Proof. Similar to the proof of Theorem 1, we define the weighted adjacency matrix $M(n_i)$ as follows:

$$M(n_i) = \begin{pmatrix} 0 & x^{3+n_i-2} & 0 & x^{2+n_i-2} & 0 \\ 0 & x^{3+n_i-2} & 0 & x^{2+n_i-2} & 0 \\ 0 & x^{3+n_i-2} & 0 & x^{2+n_i-2} & 0 \\ x^{3+n_i-2} & (n_i-1)x^{3+n_i-1} & x^{4+n_i-2} & (n_i-1)x^{2+n_i-1} & x^{3+n_i-2} \\ x^{3+n_i-2} & (n_i-1)x^{3+n_i-1} & x^{4+n_i-2} & (n_i-1)x^{2+n_i-1} & x^{3+n_i-2} \end{pmatrix}.$$

By Corollary 4, it suffices to compute the sum of the main diagonal entries of the matrix $(M(n_1)\cdot M(n_2)\cdot M(n_3))^2$. Through matrix multiplication, we obtain

$$\begin{aligned} \operatorname{tr}((M(n_1)\cdot M(n_2)\cdot M(n_3))^2) = {} & 2x^{2(n_1+n_2+n_3)+3} + (n_1+n_2+n_3+3)^2 x^{2(n_1+n_2+n_3)+4} \\ & + 2(n_1+1)(n_2+1)(n_3+1)(n_1+n_2+n_3+3)x^{2(n_1+n_2+n_3)+5} \\ & + (n_1+1)^2(n_2+1)^2(n_3+1)^2 x^{2(n_1+n_2+n_3)+6}. \end{aligned}$$

This completes the proof. □

Given a parallelogram $\overline{D}$, a *corona of* $\overline{D}$ is a lozenge tiling along the edges of $\overline{D}$ without utilizing any additional lozenges. The number of coronas of a parallelogram $\overline{D}$ is denoted by $\overline{D}(n_1, n_2)$.

Theorem 8. *Let $n_1, n_2 \in \mathbb{N}$, and let $\overline{D}(n_1, n_2)$ denote the number of coronas of a $\overline{D}$. Then, the number of lozenges in a corona of $\overline{D}$ can only take four values: $2(n_1+n_2)+3$, $2(n_1+n_2)+4$, $2(n_1+n_2)+5$, and $2(n_1+n_2)+6$. For $1 \le i \le 4$, let $\overline{d}_i(n_1, n_2)$ denote the number of corona tilings with $2(n_1+n_2)+2+i$ lozenges. Then we have*

$$\overline{d}_1(n) = 2, \qquad \overline{d}_3(n) = 2(n_1+1)(n_2+1)(n_1+n_2+3),$$
$$\overline{d}_2(n) = (n_1+n_2+3)^2, \qquad \overline{d}_4(n) = (n_1+1)^2(n_2+1)^2.$$

Furthermore, we obtain

$$\overline{D}(n_1, n_2) = \sum_{i=1}^{4} \overline{d}_i(n) = \big((n_1+1)(n_2+1) + (n_1+n_2+3)\big)^2 + 2.$$

Proof. Similar to the proof of Theorem 2, we define the following two weighted adjacency matrices $\overline{R}$ and $\overline{T}$:

$$\overline{R} = \begin{pmatrix}
(n_1-1)x^{2+n_1-1} & x^{3+n_1-2} & x^{3+n_1-2} & (n_1-1)x^{3+n_1-1} & x^{4+n_1-2} \\
(n_1-1)x^{2+n_1-1} & x^{3+n_1-2} & x^{3+n_1-2} & (n_1-1)x^{3+n_1-1} & x^{4+n_1-2} \\
(n_1-1)x^{2+n_1-1} & x^{3+n_1-2} & x^{3+n_1-2} & (n_1-1)x^{3+n_1-1} & x^{4+n_1-2} \\
x^{2+n_1-2} & 0 & 0 & x^{3+n_1-2} & 0 \\
x^{2+n_1-2} & 0 & 0 & x^{3+n_1-2} & 0 \\
x^{2+n_1-2} & 0 & 0 & x^{3+n_1-2} & 0 \\
x^{2+n_1-2} & 0 & 0 & x^{3+n_1-2} & 0 \\
x^{2+n_1-2} & 0 & 0 & x^{3+n_1-2} & 0
\end{pmatrix},$$

and

$$\overline{T} = \begin{pmatrix}
(n_2-1)x^{n_2+2} & x^{n_2+1} & x^{n_2+2} & (n_2-1)x^{n_2+2} & x^{n_2+2} & x^{n_2+2} & (n_2-1)x^{n_2+3} & x^{n_2+3} \\
(n_2-1)x^{n_2+2} & x^{n_2+1} & x^{n_2+2} & (n_2-1)x^{n_2+2} & x^{n_2+2} & x^{n_2+2} & (n_2-1)x^{n_2+3} & x^{n_2+3} \\
x^{n_2+1} & 0 & 0 & x^{n_2+1} & 0 & 0 & x^{n_2+2} & 0 \\
x^{n_2+1} & 0 & 0 & x^{n_2+1} & 0 & 0 & x^{n_2+2} & 0 \\
x^{n_2+1} & 0 & 0 & x^{n_2+1} & 0 & 0 & x^{n_2+2} & 0
\end{pmatrix}.$$

By Corollary 4, it follows that we only need to compute the trace of the matrix $(\overline{R} \cdot \overline{T})^2$. Performing the matrix multiplication, we obtain

$$\begin{aligned}
\operatorname{tr}((\overline{R} \cdot \overline{T})^2) = {} & 2x^{2n_1+2n_2+3} + (n_1+n_2+3)^2 x^{2n_1+2n_2+4} \\
& + 2(n_1+1)(n_2+1)(n_1+n_2+3)x^{2n_1+2n_2+5} + (n_1+1)^2(n_2+1)^2 x^{2n_1+2n_2+6}.
\end{aligned}$$

This completes the proof. □

Note that the parallelogram case is a special case of the centrally symmetric hexagon case. Specifically, a parallelogram can be viewed as a centrally symmetric hexagon with its n_3-sides collapsed, i.e., when $n_3 = 0$. Theorem 8 is thus a corollary of Theorem 7.

5 Acknowledgments

The authors thank the anonymous referee for valuable suggestions that improved the manuscript. They would also like to show their sincere appreciation for all suggestions to improve the presentation of this paper. The second author congratulates his senior colleagues Xinyu Xu, Chen Zhang, and Zihao Zhang on the successful completion of their Ph.D. degrees in June 2025. The third author was supported by the National Natural Science Foundation of China (Grant No. 12571355).

References

[1] M. Ciucu, T. Eisenkölbl, C. Krattenthaler, and D. Zare, Enumeration of lozenge tilings of hexagons with a central triangular hole, *J. Combin. Theory Ser. A* **95** (2001), 251–334.

[2] M. Ciucu and T. Lai, Lozenge tilings of doubly-intruded hexagons, *J. Combin. Theory Ser. A* **167** (2019), 294–339.

[3] M. Ciucu, T. Lai, and R. Rohatgi, Tilings of hexagons with a removed triad of bowties, *J. Combin. Theory Ser. A* **170** (2020), 105359.

[4] M. Fulmek, A simple explanation for the "shuffling phenomenon" for lozenge tilings of dented hexagons, *Discrete Math.* **344** (2021), 112396.

[5] E. H. Kuo, Applications of graphical condensation for enumerating matchings and tilings, *Theoret. Comput. Sci.* **319** (2004), 29–57.

[6] T. Lai, Enumeration of tilings of quartered Aztec rectangles, *Electron. J. Combin.* **21** (2014), P4.46.

[7] T. Lai, A new proof for the number of lozenge tilings of quartered hexagons, *Discrete Math.* **338** (2015), 1866–1872.

[8] T. Lai, A q-enumeration of lozenge tilings of a hexagon with three dents, *Adv. in Appl. Math.* **82** (2017), 23–57.

[9] T. Lai, A shuffling theorem for reflectively symmetric tilings, *Discrete Math.* **344** (2021), 112390.

[10] T. Lai and R. Rohatgi, Enumeration of lozenge tilings of a hexagon with a shamrock missing on the symmetry axis, *Discrete Math.* **342** (2019), 451–472.

[11] T. Lai and R. Rohatgi, Tiling generating functions of halved hexagons and quartered hexagons, *Ann. Comb.* **25** (2021), 471–493.

[12] R. Rohatgi, Enumeration of lozenge tilings of halved hexagons with a boundary defect, *Electron. J. Combin.* **22** (2015), #P4.22.

[13] N. J. A. Sloane et al., *The On-Line Encyclopedia of Integer Sequences*, 2025. Available at https://oeis.org.

[14] R. P. Stanley, *Algebraic Combinatorics: Walks, Trees, Tableaux, and More*, 2nd edition. Undergraduate Texts in Mathematics. Springer, 2018.

[15] R. P. Stanley, *Enumerative Combinatorics*, Vol. 1, 2nd edition. Cambridge Studies in Advanced Mathematics, Vol. 49, Cambridge University Press, 2012.

2020 *Mathematics Subject Classification*: Primary 05A15; Secondary 05B45.
Keywords: lozenge tiling, walk in a graph, adjacency matrix, generating function.

(Concerned with sequences A380346 and A380416.)

Received November 19 2025; revised versions received December 3 2025; December 5 2025. Published in *Journal of Integer Sequences*, December 5 2025.

Return to Journal of Integer Sequences home page.